New Journal of Physics
An Institute of Physics and Deutsche Physikalische Gesellschaft Journal

Single molecule force spectroscopy by AFM indicates helical structure of poly(ethylene-glycol) in water

F Oesterhelt, M Rief and H E Gaub

Ludwig-Maximilians-Universität München, Lehrstuhl für Angewandte Physik, Amalienstraße 54, 80799 München, Germany
E-mail: Filipp.Oesterhelt@physik.uni-muenchen.de

New Journal of Physics **1** (1999) 6.1–6.11 (http://www.njp.org/)
Received 10 November 1998; online 24 March 1999

Abstract. We elongated individual poly(ethylene-glycol) PEG molecules tethered at one end to an AFM cantilever. We observed the resistive force as a function of elongation in different solvents. In all cases the molecular response was found to be fully reversible and thus in thermodynamic equilibrium. In hexadecane the stretched PEG acts like an ideal entropy spring and can be well described as a freely jointed chain. In water we observed marked deviations in the transition region from entropic to enthalpic elasticity, indicating the deformation of a supra-structure within the polymer. An analysis based on elastically coupled *Markovian* two-level systems agrees well with recent *ab initio* calculations predicting that PEG in water forms a non-planar supra-structure which is stabilized by water bridges. We obtained a binding free energy of $3.0 \pm 0.3\ kT$.

1. Introduction

AFM [2] has become an extremely versatile tool for a broad range of problems, particularly in materials and life sciences. The ability to apply and measure tiny forces between tip and sample now extends beyond imaging into applications ranging from measuring colloidal forces [4, 9] to monitoring enzymatic activity in individual proteins [20].

Force spectroscopy by AFM has been used to measure the binding forces of different receptor–ligand systems [15, 18], observe reversible unfolding of protein domains [19, 23] and investigate polysaccharide elasticity at the level of inter-atomic bond flips [24]. Here, we describe force spectroscopy experiments involving the polymer poly(ethylene-glycol) (PEG). We stretched single polymers with an AFM cantilever and measured polymer extension in different solvents as a function of applied load (see figure 1).

1367-2630/99/000006+11$19.50

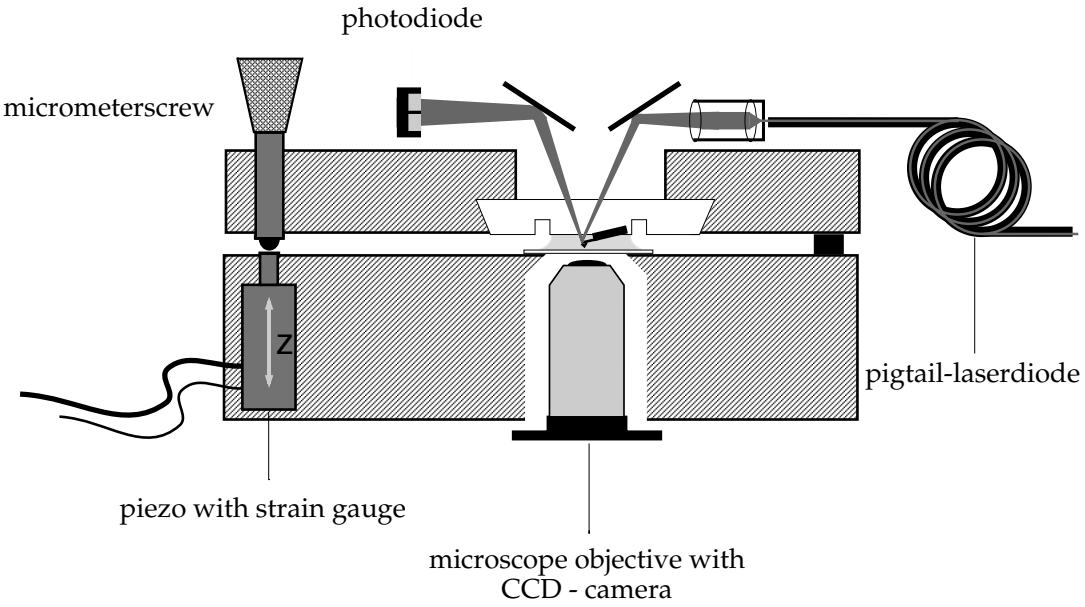

Figure 1. Schematic of the experimental set-up.

PEG is a water soluble polymer with a broad range of technical applications [12]. It serves as a thickening agent or additive to detergents and cosmetics [17]. PEG-modified surfaces resist protein adsorption, e.g. in stealth liposomes [3]. PEG-modification of protein is used to change solubility or provide a surface-linking tether [13]. In biochemistry it is also used as a fusogene for membranes [16]. Most of these properties derive from its high affinity for water. Via the dipoles of the oxygen atoms, PEG can bind water up to its own weight, i.e. 2.5 water molecules per monomer unit [12].

PEG is commercially available with a molecular weight of up to several megadaltons corresponding to a contour length of up to several μm, making it accessible to single-molecule force spectroscopy. In the crystalline state PEG assumes a helical conformation [27]. IR spectroscopy shows that it might keep this structure at least partially when dissolved in water [1]. The experiments presented here confirm the helical superstructure of PEG and show the contributions of water to its stabilization.

2. Experimental

2.1. Single molecule force spectrometer

The home-built spectrometer (figure 1), while based on AFM technology, is optimized for resolution orthogonal to the specimen plane; x–y translation occurs manually. The instrument contains two massive aluminum bars, forced together with a spring blade and opened by a stack piezo with built-in strain gauge. We mounted the sample and cantilever on opposing sides of the clamp. Optics to detect tip deflection were fixed on the upper block, together with the cantilever. To minimize pointing instability and the resulting artifact in the a–b signal, we coupled the light into the optics via monomode fibre. We adjusted the laser spot size so as to just fill the cantilever, thus preventing unwanted interference from obscuring the baseline force measurement. The tip

and sample were observed through a microscope objective with a CCD camera. The cantilever holder was made of plexiglass. In most cases the use of O-rings was not necessary as the liquid drop was kept between holder and sample by surface tension. Actuation and data acquisition were performed with 16-bit resolution. Typically 4 k datapoints per scan were taken. The scan speed could be varied between 5 nm s^{-1} and 30 μm s^{-1}.

Pre-functionalized tips require care to prevent tip–surface contact before the onset of force measurements. To avoid this, we introduced a new approach mode, using the hydrodynamic drag as a control parameter. Continuous force curves (without contact) were measured at 80% of the z-piezo extension while a motor pushed the blocks together via a μm-screw. Hysteresis between approach and retract curves increased dramatically as the tip neared the surface. By observing this, we could approach safely without unwanted contact between tip and sample before we executed the first force curve.

2.2. Calibration

Silicon-nitride cantilevers from Digital Instruments (DI, Santa Barbara, CA) and PARK Scientific Instruments (PARK, Sunnyvale, CA) were used for all force measurements. Each lever was calibrated after a given experiment using the equipartition method, using the rms thermal diffusion of the tip to compute its spring constant [5, 11]. The measured spring constants of the cantilevers varied between 60 and 100 mN m^{-1} (Digital Instruments) and 6 and 7 mN m^{-1} (PARK Scientific Instruments) respectively. The strain gauge that measures the z-movement was calibrated interferometrically, taking advantage of the weak interferences of the laser which cause an oscillation of the detector signal over the z displacement [14].

2.3. Sample preparation

Custom synthesized PEG (molecular weight of approximately 30.000 from SHEARWATER, Huntsville, Alabama) with a thiol group at one end and a butoxy group at the other end was used for this study. We deposited a drop of 1 mM PEG solution in Millipore water onto a freshly evaporated gold surface and allowed the surface to dry at 55°C. The sample was then rinsed with water and immediately used for experiments. Force spectroscopy was carried out in either phosphate-buffered saline (PBS, SIGMA, Deisenhofen, Germany, PH 7.4, 130 mM NaCl) or in hexadecane (FLUKA, Neu-Ulm, Germany).

Several techniques have been reported for the coupling of single molecules to the tip [7, 13, 26]. Adsorption has been established as the most versatile approach giving rise to stable attachment against hundreds of piconewton over tens of seconds without creeping [19, 21, 23, 24, 25]. In the experiments reported here the tip was moved toward the surface until contact occurred (figure 2(a)). It was then kept there for up to several seconds, allowing the polymer to adsorb (figure 2(b)). The adsorbed polymer was then stretched by retracting the tip (figure 2(c)). In cases where multiple polymers had bound, the tip was gradually withdrawn from the surface until all but the longest polymer ruptured (figure 3, first trace).

Once we confirmed single-molecule attachment, we kept the tip away from the polymer brush on the surface to prevent added polymer adsorption. The attached molecule could be stretched and relaxed repeatedly. We further confirmed that a single molecule had been measured by observing that its rupture ended all probe–surface interaction (figure 3, last trace).

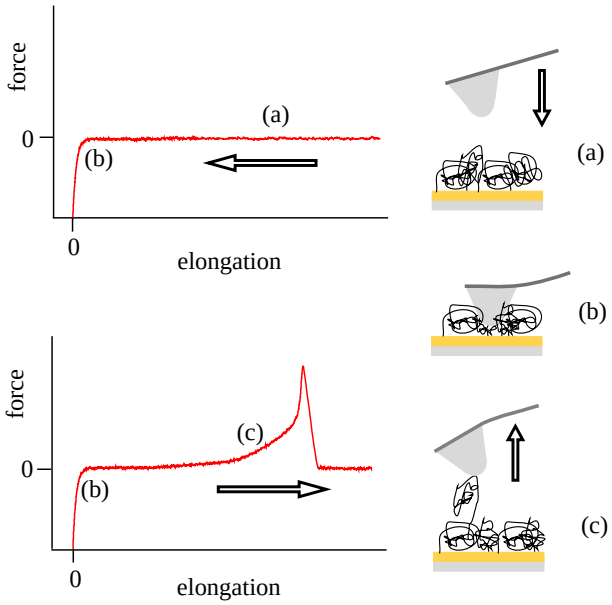

Figure 2. Schematic of a single molecule force spectroscopy experiment. Upon approach of the AFM cantilever to the grafted polymer film (a) a gradually increasing repulsion is measured at distances that are on the order of the radius of gyration of the polymer (b). If the tip is indented further individual polymers are picked up by either adsorption or bonding. Upon retraction of the cantilever the polymer is stretched while force and elongation are recorded (c).

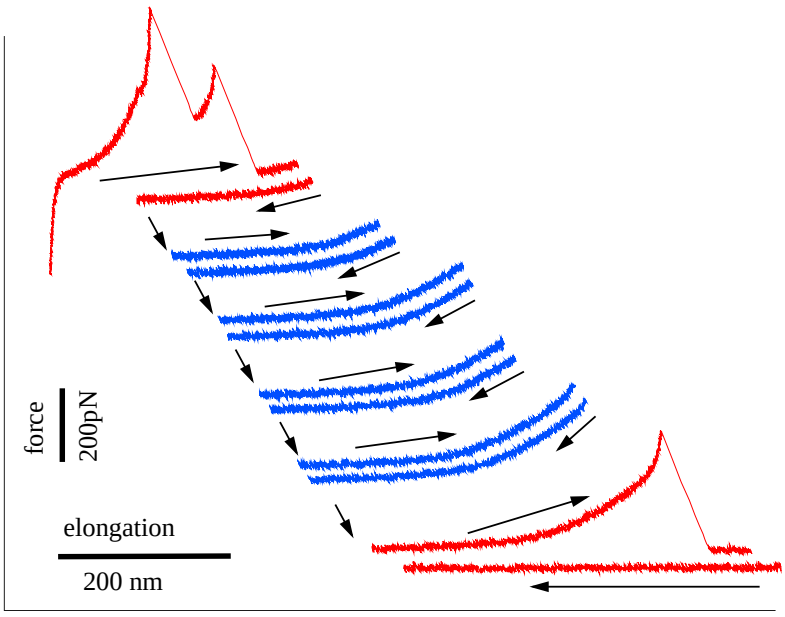

Figure 3. Reversible extension of PEG. At first contact three molecules had attached to the tip. During the first extension two of them ruptured or detached. The remaining molecule was repeatedly stretched. In the last scan the force was increased beyond rupture.

3. Results

Figures 4(a) and 4(b) show single-molecule PEG extension traces recorded in PBS and hexadecane respectively. Since tip and surface attachments can occur anywhere along the polymer, the length of polymer stretched between tip and sample varies, as evidenced by different scales of extension curves in both figures. When normalized by contour length, all traces taken in a given solvent superimpose within experimental noise limits (figure 5). Since standard polymer theories predict the restoring force scales linearly with contour length [8, 10], this observation further supports the idea that the traces reflect single molecules. Moreover, it provides a criterion for differentiating between single- and multiple-molecule contacts.

PEG force-extension traces from both solvents superimpose in the low force regime, reflecting not molecule-specific properties but statistical behaviour of an ideal polymer. Traces in both solvents also superimpose at very high forces, where deformation is dominated by the stiffness of bond angle potentials and presumably independent of solvent [24]. It is in the intermediate force regime that behaviour in the two solvents will differ. Under 100 pN, PEG in water shows only 80% the elongation seen in hexadecane. This indicates the presence of solvent-mediated polymer supra-structure.

4. Discussion

4.1. PEG in apolar solvent: extended freely jointed chain model

In previous studies, we and others have shown that the stretching of single polymers is well described by an extended Langevin function [23, 26]. Entropic elasticity dominates the low force regime, described by a freely jointed chain model [10]. At high forces, bond angle torsion and bend give rise to a molecule-specific segment elasticity. Since hexadecane is entirely apolar, solvent-mediated supra-molecular assemblies are unlikely to form as well as solvent mediated intrachain interactions can be neglected. The extended Langevin function is thus an appropriate description of the polymer.

$$L(F) = L_{\mathrm{C}}(F) \cdot \left(\coth\left(\frac{F \cdot L_{\mathrm{K}}}{k_{\mathrm{B}} \cdot T} \right) - \frac{k_{\mathrm{B}} \cdot T}{F \cdot L_{\mathrm{K}}} \right) + N_{\mathrm{S}} \cdot \frac{F}{K_{\mathrm{S}}} \tag{1}$$

Here F reflects the applied force, N_{S} the total number of segments, k_{B} the Boltzmann constant and T the temperature. The contour length L_{C} determines the overall length scale of the force-extension curve. The Kuhn length L_{K} determines the slope in the low-force regime and the curvature in the mid-force regime, while the segment elasticity K_{S} determines the slope in the high-force regime. From fitting the superimposed traces (see figure 5, solid line) we obtain a Kuhn length L_{K} of 7 Å and a segment elasticity K_{S} of 150 N m^{-1} per monomer. At forces around 50 pN small but still detectable deviations from pure entropic elasticity are measurable. These deviations indicate the deformation of a slight suprastructure which may be caused by the interaction of the oxygen atoms within the chain or with residual water.

4.2. Water bridges: elastically coupled two-level systems

When dissolved in aqueous environment the deformation curves of PEG deviate markedly from the ones measured in hexadecane. No combination of parameters in the extended FJC model fits the data over the whole range. The marked deviations in the mid-force regime indicate

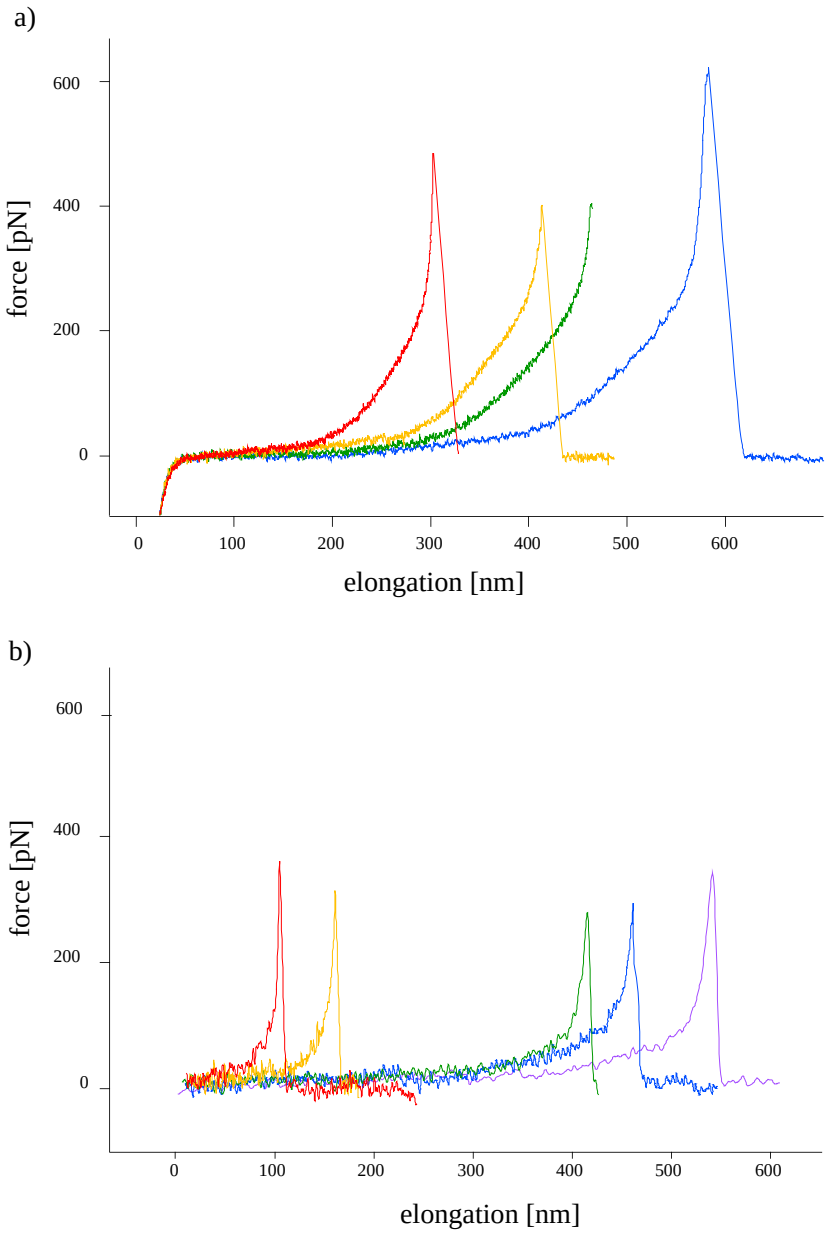

Figure 4. Extension traces of individual PEG molecules of different length in PBS (a) and hexadecane (b).

conformational rearrangements of a water-dependent supramolecular structure as a result of the applied force.

In the crystalline state PEG strands arrange in parallel, each in a helical form. The sinuousness of the helix is 2/7 and the bonds of the C–O–C–. . . backbone are folded in a trans-trans-gauche (ttg) order. This results in a mean monomer length of 2.78 Å [27].

Begum and Matsuura [1] showed that the gauche state of the C–C bond, which is typical for the crystaline helical state, is retained when PEG is dissolved in water. Applied tension could drive a transition from a helix to an all-trans configuration, energetically less favourable in the

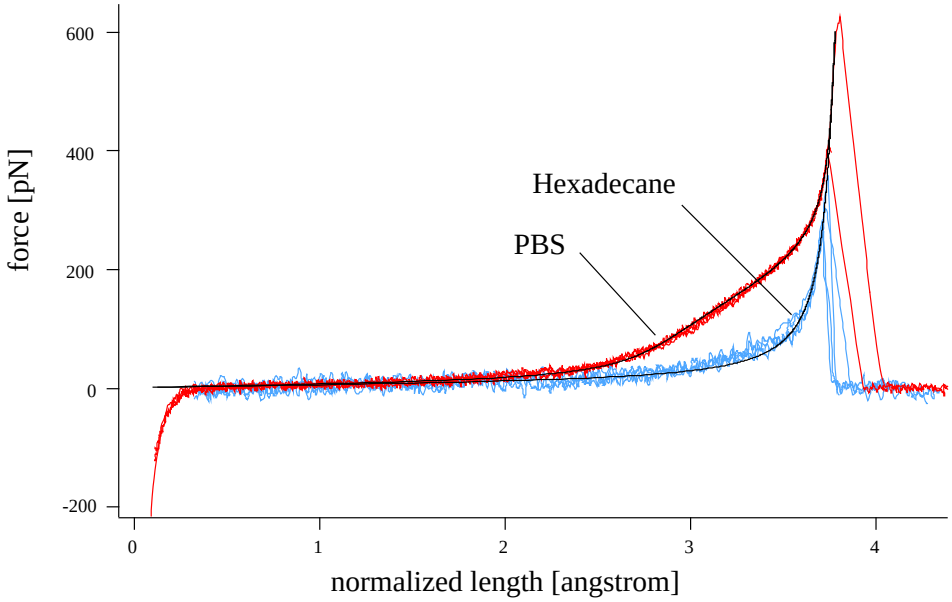

Figure 5. Superposition of the extension traces shown in figure 4 after normalization of their contour length. The solid line shows the best fit to the models.

absence of strain. Since the measured deformation curves of PEG are fully reversible (figure 6) we can assume that the processes of this transition occur much faster than our experimental time scale. This conformational transition can therefore be modelled by a Markovian two-level system in equilibrium [6, 22]. In this model, every monomer can exist either in the trans-trans-trans (ttt) or ttg conformation with a difference in Gibbs free energy ΔG and a length difference ΔL (figure 7). Stretching then shifts the equilibrium away from the shorter helical state and toward the elongated planar state. The total contour length is then given by

$$L_{\mathrm{C}} = N_{\mathrm{planar}} \cdot L_{\mathrm{planar}} + N_{\mathrm{helical}} \cdot L_{\mathrm{helical}}$$

The ratio of the populations $N_{\mathrm{helical}}/N_{\mathrm{planar}}$ is Boltzmann distributed:

$$\frac{N_{\mathrm{helical}}}{N_{\mathrm{planar}}} = \mathrm{e}^{+\Delta G/k_{\mathrm{B}}T}$$

The applied force alters the difference in free energy according to:

$$\Delta G(F) = (G_{\mathrm{planar}} - G_{\mathrm{helical}}) - F \cdot (L_{\mathrm{planar}} - L_{\mathrm{helical}})$$

Together with equation (1) this results in the following extension-force relation:

$$L(F) = N_{\mathrm{S}} \cdot \left(\frac{L_{\mathrm{planar}}}{\mathrm{e}^{-\Delta G/k_{\mathrm{B}}T} + 1} + \frac{L_{\mathrm{helical}}}{\mathrm{e}^{+\Delta G/k_{\mathrm{B}}T} + 1} \right) \cdot \left(\coth\left(\frac{F \cdot L_{\mathrm{K}}}{k_{\mathrm{B}} \cdot T} \right) - \frac{k_{\mathrm{B}} \cdot T}{F \cdot L_{\mathrm{K}}} \right) + N_{\mathrm{S}} \cdot \frac{F}{K_{\mathrm{S}}} \quad (2)$$

The PEG force-extension traces measured in PBS were fit to equation (2). We applied the values for the Kuhn length L_{K} and segment elasticity K_{C} measured in hexadecane. We estimate the ttt state length as a zigzag backbone with bond lengths of 1.54 Å for the C–C bond, 1.43 Å for the C–O bond, and tetrahedral angles, giving a net length of 3.58 Å. Best fit parameters (see figure 5, solid line) include a free energy difference of $3 \pm 0.3\ kT$ and a ttg length of 2.8 ± 0.05 Å.

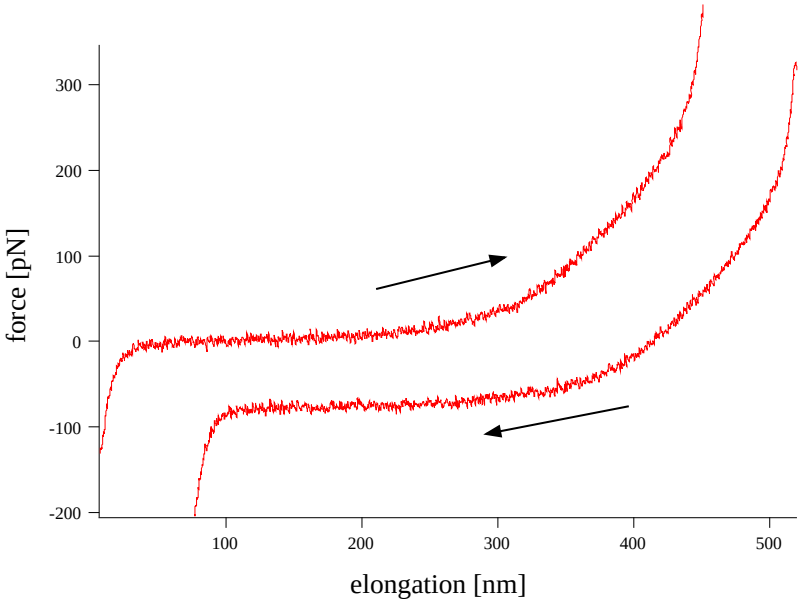

Figure 6. Reversible extension of a PEG molecule. For clarity the traces are offset.

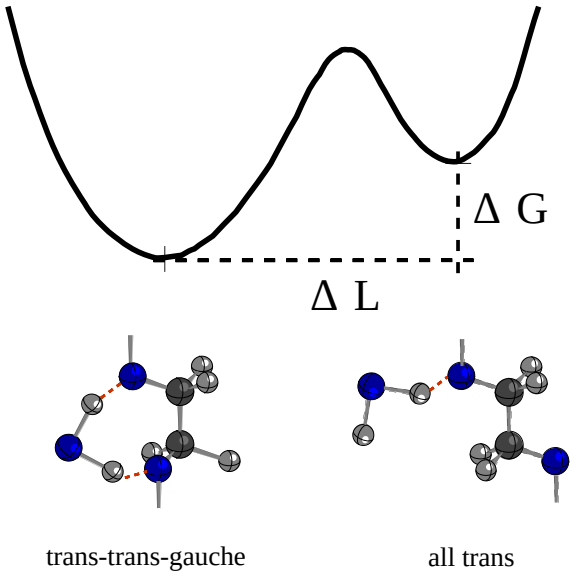

Figure 7. Elastically coupled two-level system as model for PEG elasticity.

Figure 8 illustrates the accuracy of these fits. Figure 8(a) shows an expanded fit to the PBS force-extension curve in the low force-regime. The solid lines show fits with above parameters but different Kuhn lengths. In figure 8(b) we vary the free energy difference and length difference between the two conformations.

The ttg segment length estimate of 2.80 ± 0.1 Å agrees well with the crystallographically measured length of the helical ttg conformatoin, 2.78 Å [27]. This finding confirms that PEG retains a ttg structure in water, consistent with IR spectroscopy measurements that suggest a

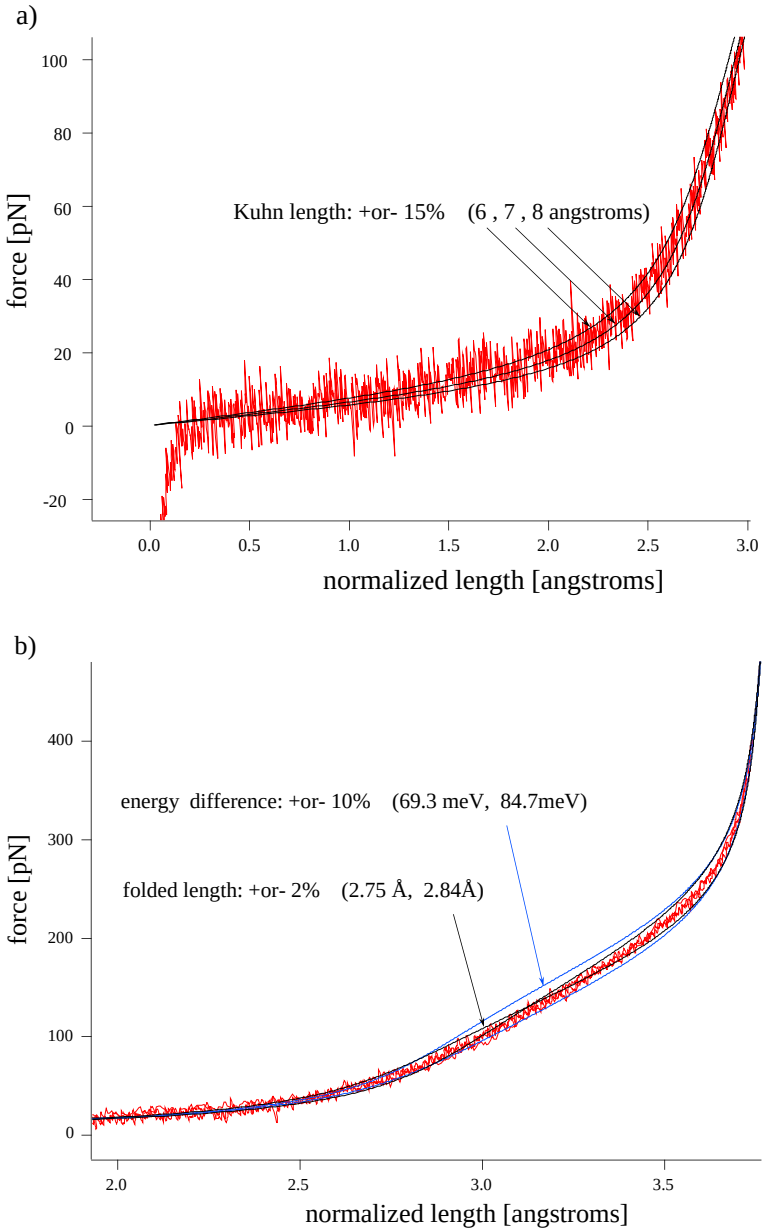

Figure 8. Best fits of PEG extension curves in water (a) in the low-force regime for different Kuhn lengths and (b) in the mid-force regime for different energies and ttg-lengths respectively.

dynamic helical structure [1].

Ab initio QM calculations of Wang *et al* [28] show marked differences in the hydration of the PEG backbone in the different configurations. In ttg, a given water molecule can form hydrogen bonds with two adjacent oxygens of the PEG, and water may thus form bridges that stabilize the helical configuration. In ttt, the distance between oxygen atoms is large enough that a water molecule may form only one hydrogen bond to the polymer backbone. The resulting net enthalpy difference between the two configurations was calculated to be $6\ kT$. Since a second

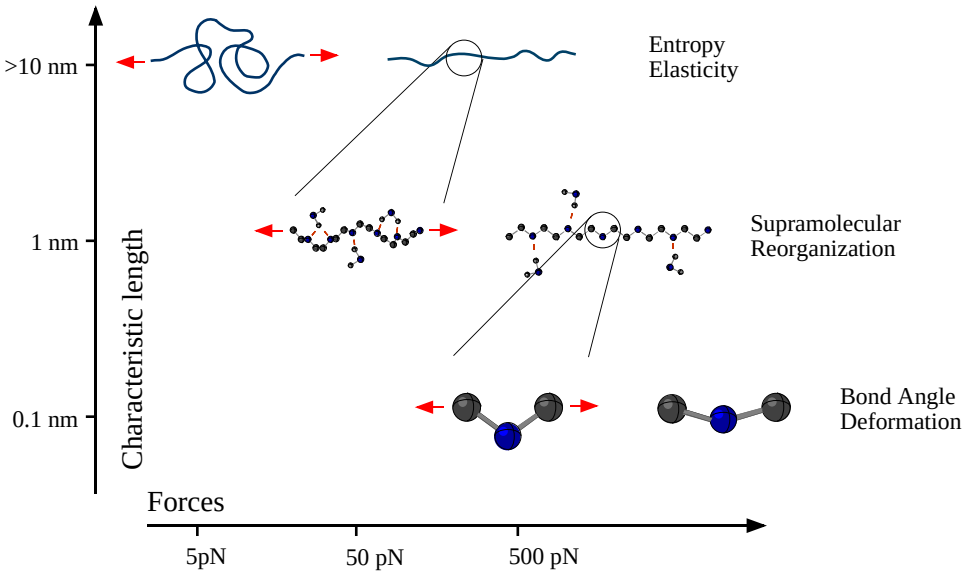

Figure 9. Schematics of the hierarchy of elastic responses in PEG.

hydrogen bond will further restrict the mobility of water, the ttt configuration enjoys an entropic advantage. Both of these factors combine to explain the measured ΔG.

5. Concluding remarks

PEG extension can be cast as a succession of three phenomena (figure 9). At forces around a few pN, entropic restoring forces explain the response. At hundreds of pN, the elasticity is purely enthalpic, explained by bond distortion. Between these extremes, one finds evidence of solvent-mediated suprastructure. Water molecules likely form fluctuating intramolecular bridges, shortening the net polymer length and resisting further extension. Since the effects of these monomer changes on polymer properties are additive, they can be measured with high precision by single-molecule force spectroscopy. Hence, described experiments can generalize to a range of biopolymers with more complex superstructure, such as proteins or polynucelotides.

Acknowledgments

Stimulating and fruitful discussions with M Grunze, B Heymann, H Grubmüller and P Schulz-Vanheyden are gratefully acknowledged. We thank A Mehta for helpful comments on the manuscript.

References

[1] Begum R and Matsuura H 1997 Conformational properties of short poly(oxyethylene) chains in water studied by IR spectroscopy *J. Chem. Soc. Faraday Trans.* **93** 3839–48
[2] Binnig G, Quate C F and Gerber C 1986 Atomic force microscope *Phys. Rev. Lett.* **56** 930
[3] Blume G, Cevc G, Crommelin M D, Bakker-Woudenberg I A, Kluft C and Storm G 1993 Specific targeting with poly(ethylene glycol)-modified liposomes: coupling of homing devices to the ends of the polymeric

chains combines effective target binding with long circulation times. *Biochim. Biophys. Acta.* **1149** (1) 180–4

[4] Butt H-J 1991 Measuring electrostatic, van der Waals, and hydration forces in electrolyte solutions with an atomic force microscope *Biophys. J.* **60** 1438–44

[5] Butt H-J and Jaschke M 1995 Thermal noise in atomic force microscopy *Nanotechnology* **6** 1–7

[6] Cluzel P, Lebrun A, Heller C, Lavery R, Viovy J-L , Chateny D and Caron F 1996 DNA: an extensible molecule *Science* **271** 792–4

[7] Dammer U, Hegner M, Anselmetti D, Wagner P, Drier M, Huber W and Güntherodt H-J 1994 Specific antigen/antibody interactions observed by atomic force microscopy *Biophys. J.* **70** 2437–41

[8] Doi M and Edwards S F 1995 *The Theory of Polymer Dynamics* (Oxford: Clarendon)

[9] Ducker W A, Senden T J and Pashley R M 1991 Direct measurement of colloidal forces using an atomic force microscope *Nature* **353** 239–41

[10] Flory P J 1988 *Statistical Mechanics of Chain Molecules* (München: Hanser)

[11] Florin E L, Rief M, Lehmann H, Ludwig M, Dornmair C, Moy V T and Gaub H E 1995 Sensing specific molecular interactions with the atomic force microscope *Biosensors and Bioelectronics* **10** 895–901

[12] Harris J M 1992 *Poly(ethylene glycol)* (New York: Plenum)

[13] Hinterdorfer P, Baumgartner W, Gruber H J, Schilcher K and Schindler H 1996 Detection and localization of individual antibody-antigen recognition events by atomic force microscopy *Proc. Natl. Acad. Sci. USA.* **93** 3477–81

[14] Jaschke M and Butt H-J 1995 Height calibration of optical lever atomic force microscopes by simple laser interferometry *Rev. Sci. Instrum.* **66** 1258–9

[15] Lee G U, Kidwell D A and Colton R J 1994 Sensing discrete streptavidin biotin interactions with the atomic force microscope *Langmuir* **10** 354–7

[16] Lentz B R 1994 Polymer-induced membrane fusion: potential mechanism and relation to cell fusion events *Chem. Phys. Lipids* **73** (1–2) 91–106

[17] Mark H F 1986 *Encyclopedia of Polymer Science and Engineering* (New York: Wiley)

[18] Moy V T, Florin E L and Gaub H G 1994 Intermolecular forces and energies between ligands and receptors *Science* **266** 257–9

[19] Oberhauser A F, Marszalek P E, Erickson H P and Fernandez J M 1998 The molecular elasticity of the extracellular matrix protein tenascin *Nature* **393** 181–5

[20] Radmacher M, Fritz M, Hansma H G and Hansma P K 1994 Direct observation of enzyme activity with the atomic force microscope *Science* **265** 1577–9

[21] Rief M, Clausen-Schaumann H and Gaub H E 1999 Sequence dependent mechanics of single DNA-molecules *Nat. Struct. Biol.* in press

[22] Rief M, Fernandez J M and Gaub H E 1998 Elastically coupled two-level-systems as a model for biopolymer extensibility *Phys. Rev. Lett.* **81** 4764–7

[23] Rief M, Gautel M, Oesterhelt F, Fernandez J M and Gaub H E 1997 Reversible unfolding of individual titin Ig-domains by AFM *Science* **276** 1109–12

[24] Rief M, Oesterhelt F, Heymann B and Gaub H E 1997 Single molecule force spectroscopy on polysaccharides by AFM *Science* **275** 1295–8

[25] Rief M, Pascual J, Saraste M and Gaub H E 1999 Single molecule force spectroscopy of spectrin repeats: low unfolding forces in helix bundles *Molec. Biol.* **286** 553–61

[26] Smith S B, Cui Y and Bustamante C 1996 Overstretching B-DNA: the elastic response of individual double-stranded and single-stranded DNA molecules *Science* **271** 795–8

[27] Tadokoro H 1990 *Structure of Crystalline Polymers* (Malabar: Kriege)

[28] Wang R L C, Kreuzer H J and Grunze M 1997 Molecular conformation and solvation of oligo(ethylene glycol) terminated self-assembled monolayers and their resistance to protein adsorption *J. Phys. Chem.* B **101** 9767–73